

12th National Conference
on Earthquake Engineering
Salt Lake City, Utah
27 June - 1 July 2022

Hosted by the Earthquake Engineering Research Institute

Unsegmented long-term time-dependent modeling of the Nankai subduction zone (Japan)

S. Iacoletti¹, G. Cremen², U. Tomassetti³ and C. Galasso⁴

ABSTRACT

The authors have recently presented a harmonized framework that unifies state-of-the-art methodologies for relaxing fault segmentation assumptions, including time-dependent earthquake occurrence and accounting for fault interaction. This framework has so far only been applied to shallow crustal faults, which are the typical focus of recent advancements in fault-based probabilistic seismic hazard analysis (PSHA). The methodological study presented in this paper is a first attempt to extend this framework to a subduction zone. The case study presented herein concerns the 900-km long Nankai subduction zone in South Japan. This work highlights several challenges with implementing the considered framework to subduction zones, emphasizing possible future research efforts that could improve the results presented in this study. In particular, it is concluded that (1) down-dip discretization of subduction zones should be used along with the along-strike discretization currently used for shallow crustal faults; (2) further research is needed to develop a standard physically-motivated approach to generate viable ruptures for subduction zones; (3) plate convergence rate and interplate coupling coefficients (i.e., heterogeneity of the coupling ratio defined as the slip rate divided by the plate convergence rate) should be explored and explicitly accounted for as part of the epistemic uncertainty in the hazard assessment; (4) 2D functions describing the shape of the average single-event slip should be developed.

Introduction

Fault-based probabilistic seismic hazard analysis (PSHA) has undergone significant technical and practical advancements in recent years, quickly becoming a viable assessment option in countries where a database of active faults is available [e.g., 1, 2]. Traditional PSHA approaches use earthquake catalogs to calibrate seismic sources (usually large areas) characterized by well-defined seismicity. With a fault-based approach, analysts can leverage several other sources of information (e.g., geologic and geodetic data, paleoseismic data) to better constrain the location, the occurrence rate, and the magnitude of future large earthquakes [1].

Recent advances in the field of fault-based PSHA have focused on relaxing fault segmentation assumptions [e.g., 1, 3], including time-dependent earthquake occurrence [e.g., 4], or implementing algorithms for fault interaction [e.g.,

¹ PhD Student, Department of Civil, Environmental and Geomatic Engineering, University College London, UK (salvatore.iacoletti.19@ucl.ac.uk)

² Lecturer, Department of Civil, Environmental and Geomatic Engineering, University College of London, UK (g.cremen@ucl.ac.uk)

³ Earthquake Research Analyst, Model Research and Evaluation (MRE) team, Willis Re, UK (umberto.tomassetti@willistowerswatson.com)

⁴ Professor, Department of Civil, Environmental and Geomatic Engineering, University College of London, UK, and Scuola Universitaria Superiore (IUSS) Pavia, Italy (c.galasso@ucl.ac.uk)

5]. Applications of these advances have mainly considered fault systems that comprise of shallow crustal faults.

The authors have recently unified state-of-the-art advancements in field of fault-based PSHA within a single harmonized framework [6], herein referred to as the “Iacoletti et al. framework”. The framework incorporates some underlying methodologies of the latest Uniform California Earthquake Rupture Forecast (UCERF3) [1, 4], providing a comprehensive means of relaxing fault segmentation and inferring time-dependent probabilities of mainshock occurrence. The framework also explicitly accounts for fault-interaction triggering between major known faults, using the approach outlined by Mignan et al. [5] and Toda et al. [7]. This paper presents a first attempt to adapt the Iacoletti et al. framework to a subduction zone. In particular, the case study presented herein concerns the 900-km long Nankai subduction zone in South Japan, which accommodates plate movements between the Philippines Sea Plate and the Eurasian Plate. Challenges in applying the proposed unsegmented time-dependent modeling framework to subduction zones and future prospects for research in this field are also highlighted.

Input data

The Nankai subduction zone has been extensively investigated in terms of both earthquake and tsunami risk assessments by the Japanese Headquarters For Earthquake Research Promotion (HERP) [8]. The geometry of this zone (i.e., the mesh) is available on the <https://www.j-shis.bosai.go.jp> website (last accessed 13th July 2021) and is used in this study (Fig. 1, left panel). The plate convergence rate by Hirose and Maeda [9] and the interplate coupling coefficients by Kimura et al. [10] are used in this study to compute the slip rate across the area of the subduction zone (shown in Fig. 1, left panel). However, datasets from other studies could also be integrated to account for the epistemic uncertainty in these variables.

The Nankai subduction zone has relatively long historical records and has produced several megathrust earthquakes with moment magnitude (M_W) higher than 8. These earthquakes can be either individual large events (e.g., the 1707 M_W 8.7+ event), or a combination of two relatively smaller events, occurring closely in time and space (e.g., the 1944 M_W 8.1 and the 1946 M_W 8.4). The approximate time, magnitude and geometry of major earthquakes ($M_W \geq 8$) since 684 C.E. are taken from HERP [8], Satake [11], and Fitzenz [12]. Ruptures like those of 1944 and 1946 recur the most. The 1944-type ruptures (consisting of subsections 11 and 14 or subsections 11, 14, and 17 in Fig. 1) occurred in 1096, 1361, 1498, 1854, and 1944; the 1946-type ruptures (consisting of subsections 4 and 7 in Fig. 1) occurred in 684, 1099, 1361, 1854, and 1946.

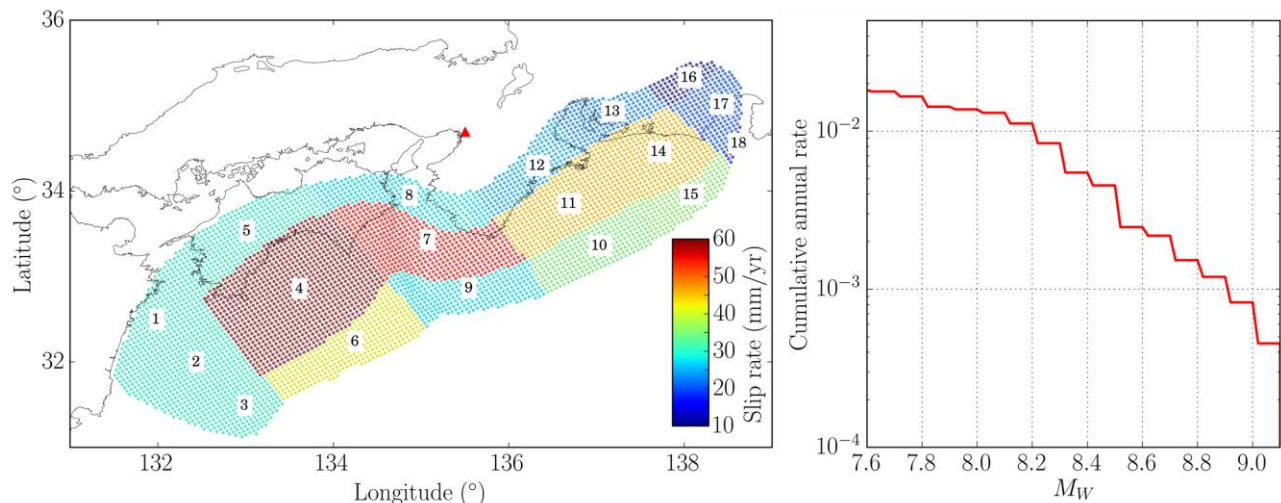


Figure 1. Left panel: the geometry of the Nankai subduction zone as modelled by HERP [8], divided into 18 subsections. The colors represent the slip rate for each section derived from the plate convergence rate by Hirose and Maeda [9] and the interplate coupling coefficients by Kimura et al. [10]. The red triangle indicates the location of Osaka. Right panel: magnitude-frequency distribution resulting from the inversion process.

Ruptures

Current physically-motivated methods to generate an ensemble of viable (i.e., physically plausible) ruptures [e.g., 13] consider only shallow crustal faults, with an along-strike discretization. Subduction zones extend much deeper than shallow crustal faults and down-dip discretization is also needed. Simple approaches could be used to create an ensemble of viable ruptures for subduction zones if the magnitude-frequency distribution (MFD) is known [e.g., 14]. However, the set of plausible ruptures must be available before performing the inversion process (see following section) that calibrates the MFD. Hence, further research is needed to develop a standard physically-motivated approach to generate viable ruptures for subduction zones. In this study, the approach by HERP [8] is adopted, which used expert judgement to divide the area of the Nankai subduction zone into 18 subsections (shown in Fig. 1, left panel) and generate a total of 80 ruptures (ranging from M_W 7.6 and 9.1). Characteristics of the ruptures, such as seismic moment M_0 and average slip D_r , were computed using formulas and recommendations in HERP [15].

Inversion

The inversion procedure of the Iacoletti et al. framework is similar to the one used by UCERF3 [1] and estimates the long-term rates f_r of the R viable ruptures by solving an optimization problem, which comprises several systems of equations, each describing a particular constraint. These constraints can be weighted by the uncertainties (e.g., standard deviations) in the data and/or by the subjective degree of belief in the importance of a particular constraint (details in [6]). The inversion constraints used in this study are (1) slip rate balancing constraint (Eq. A1 in [6]); (2) historical/paleoseismic event rate matching constraint (Eq. A4 in [6]); (3) smoothness constraint (Eq. A6 in [6]); (4) magnitude-frequency distribution (MFD) constraint (Eq. A9 in [6]); and (5) event rate constraint (not used in [6]; see Eq. 1). The slip rate balancing constraint enforces the fact that the slip D_{sr} in each rupture r that includes a given fault subsection s , multiplied by the rate f_r of that rupture, must sum to the long-term slip rate for that subsection. To obtain D_{sr} , the average slip for a given rupture D_r is spread amongst the subsections composing the rupture using the shape of the average single-event slip. One challenge of implementing this constraint for subduction zones is the fact that currently available empirical shapes of the average single-event slip are 1D along-strike functions and are only valid for shallow crustal faults. In this study, an equivalent 2D version of the tapered-slip model by Biasi et al. [16] is developed to mitigate this issue. However, further research and empirical data are needed in this regard. The historical/paleoseismic event rate matching constraint uses data from historical or paleoseismic studies to constrain the rupture rates. Consistent with [17], this constraint is only implemented for subsections that participated in at least five past events. The estimates of the mean paleoseismic event rates (along with the standard deviation of the mean observed event rate) are computed with the method proposed by Biasi et al. [18]. The smoothness constraint and the MFD constraints are applied as in [6]. For example, the Gutenberg-Richter MFD is chosen for the MFD constraint. The event rate constraint is necessary to force the rate of ruptures like those of 1944 and 1946 to be close to a specified rate of occurrence. This constraint is specific to the Nankai subduction zone and helps the solving algorithm to find solutions in agreement with past seismicity. This constraint is implemented as follows:

$$\sum_{r=1}^R \frac{G}{\sigma} f_r = \frac{f^*}{\sigma} \quad (1)$$

where f^* is the specific mean rate of occurrence for a certain subgroup of ruptures with standard deviation σ (in this study, f^* and σ were calculated with [18]), $G = 1$ if the r^{th} rupture is included in the subgroup, and all other variables are as previously defined. Fig. 1 (right panel) shows the MFD resulting from the inversion procedure.

Synthetic catalog and hazard curves

Synthetic catalogs are generated using the procedure proposed by Iacoletti et al. [6] with the following rupture occurrence models: (1) time-independent (Poissonian) model (TI); (2) time-dependent Brownian Passage Time (BPT, [17]) model (TD, see Appendix B in [6]); and (3) BPT model with fault interaction algorithm (TD-FI, see Appendix C in [6]). The synthetic catalogs comprise 100,000 1-yr long realizations of ruptures starting from 2022. For each event in the synthetic catalogs, the ground-motion is computed using the BCHydro ground-motion model [19]. Hazard

curves for peak ground acceleration (PGA) are computed with Eq. 4 in [6] for the city of Osaka (Japan, latitude: 34.69, longitude: 135.50) and shown in Fig. 3.

Fig. 3 shows that the TD hazard curve provides higher ground-motion amplitudes than the TI curve for any annual probability of exceedance. This means that the model calibrated in this study considers the Nankai subduction zone to be closer to failure than average, which is consistent with its recent history. For a single seismic source, a time-dependent occurrence model can produce larger hazard than a time-independent one if the time elapsed since the last event is higher than around 50% of the mean recurrence interval (see [6, 17]). In the case of the Nankai subduction zone, the time-independent mean recurrence interval of events with $M_W \geq 8.2$ is approximately 100 years (Fig. 1, right panel) and the most recent megathrust event occurred in 1946, such that the time elapsed since the last event is around 76 years (approximately 76% of the mean recurrence interval). For the considered case study, the inclusion of the fault interaction mechanism amongst adjacent areas of the Nankai subduction zone (TD-FI curve) results in considerably different hazard compared to that which results from using only time-dependent occurrence models (TD curve): differences in ground-motion amplitudes between the TD-FI and TD curves range from 20% to 70%, depending on the annual probabilities of exceedance. Note that the results shown in Fig. 3 only account for the Nankai subduction zone.

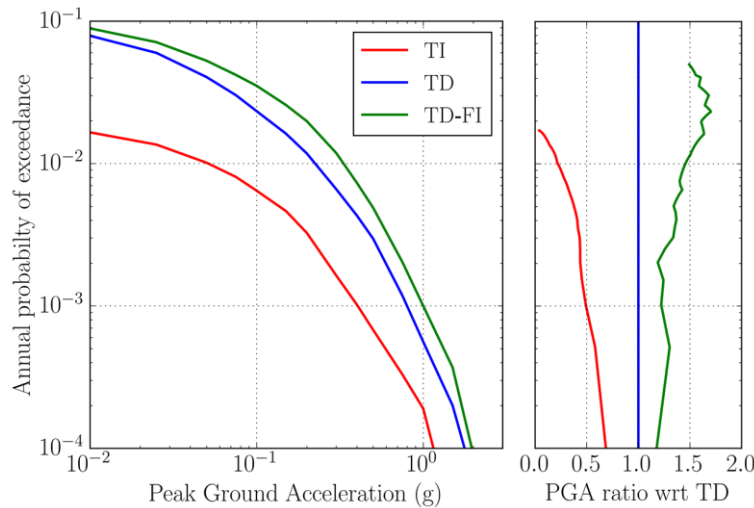


Figure 3. PGA hazard curves for the city of Osaka for TI, TD and TD-FI. The panel on the right show the ratios of the hazard curves – with respect to TD – for TD-FI and TI.

Conclusions

The unsegmented time-dependent modeling framework proposed by Iacchetti et al. [6] is a powerful tool for fault-based PSHA, but it only focuses on shallow crustal faults. This methodological study is the first attempt to extend the framework to a subduction zone and explore related challenges. The Nankai subduction zone in South Japan is used as a case study and PGA hazard curves are developed for the city of Osaka (Japan), considering only the seismicity of the Nankai subduction zone. Using different rupture occurrence models leads to considerably different hazard estimates; the time-independent model produces the lowest hazard and the time-dependent model with fault interaction mechanism results in the highest hazard. The study highlighted several challenges with implementing the framework in [6] for subduction zones. In particular, (1) down-dip discretization of subduction zones should be used along with the along-strike discretization currently used for shallow crustal faults; (2) further research is needed to develop a standard physically-motivated approach to generate viable ruptures for subduction zones; (3) plate convergence rate and interplate coupling coefficients should be explored and explicitly accounted for as part of the epistemic uncertainty in the hazard assessment; (4) 2D functions describing the shape of the average single-event slip should be developed.

Acknowledgments

The authors thank Dr Crescenzo Petrone and Dr Myrto Papaspiliou for the feedback on this study.

References

1. Field, E.H., Arrowsmith, R.J., Biasi, G.P., Bird, P., Dawson, T.E., Felzer, K.R., Jackson, D.D., Johnson, K.M., Jordan, T.H., Madden, C., Michael, A.J., Milner, K.R., Page, M.T., Parsons, T., Powers, P.M., Shaw, B.E., Thatcher, W.R., Weldon, R.J., Zeng, Y., 2014. Uniform California Earthquake Rupture Forecast, Version 3 (UCERF3) - The Time-Independent Model. *Bulletin of the Seismological Society of America* 104, 1122–1180.
2. Scotti, O., Visini, F., Faure Walker, J., Peruzza, L., Pace, B., Benedetti, L., Boncio, P., Roberts, G., 2021. Which Fault Threatens Me Most? Bridging the Gap Between Geologic Data-Providers and Seismic Risk Practitioners. *Frontiers in Earth Science* 8, 750.
3. Chartier, T., Scotti, O., Lyon-Caen, H., Boiselet, A., 2017. Methodology for earthquake rupture rate estimates of fault networks: example for the western Corinth rift, Greece. *Nat. Hazards Earth Syst. Sci.* 17, 1857–1869.
4. Field, E.H., Biasi, G.P., Bird, P., Dawson, T.E., Felzer, K.R., Jackson, D.D., Johnson, K.M., Jordan, T.H., Madden, C., Michael, A.J., Milner, K.R., Page, M.T., Parsons, T., Powers, P.M., Shaw, B.E., Thatcher, W.R., Weldon, R.J., Zeng, Y., 2015. Long-Term Time-Dependent Probabilities for the Third Uniform California Earthquake Rupture Forecast (UCERF3). *Bulletin of the Seismological Society of America* 105, 511–543.
5. Mignan, A., Danciu, L., Giardini, D., 2016. Considering large earthquake clustering in seismic risk analysis. *Nat Hazards*.
6. Iacoletti, S., Cremen, G., Galasso, C., 2021. Advancements in multi-rupture time-dependent seismic hazard modeling, including fault interaction. *Earth-Science Reviews* 220, 103650.
7. Toda, S., Stein, R.S., Reasenber, P.A., Dieterich, J.H., Yoshida, A., 1998. Stress transferred by the 1995 Mw = 6.9 Kobe, Japan, shock: Effect on aftershocks and future earthquake probabilities. *J. Geophys. Res.* 103, 24543–24565.
8. The Headquarters For Earthquake Research Promotion. Long term evaluation of seismic activity of the Nankai Trough (2nd edition), http://www.jishin.go.jp/main/chousa/kaikou_pdf/nankai_2.pdf (in Japanese).
9. Hirose, F., Maeda, K., 2013. Simulation of recurring earthquakes along the Nankai trough and their relationship to the Tokai long-term slow slip events taking into account the effect of locally elevated pore pressure and subducting ridges. *Journal of Geophysical Research: Solid Earth* 118, 4127–4144.
10. Kimura, H., Tadokoro, K., Ito, T., 2019. Interplate Coupling Distribution Along the Nankai Trough in Southwest Japan Estimated From the Block Motion Model Based on Onshore GNSS and Seafloor GNSS/A Observations. *Journal of Geophysical Research: Solid Earth* 124, 6140–6164.
11. Satake, K., 2015. Geological and historical evidence of irregular recurrent earthquakes in Japan. *Philosophical Transactions of the Royal Society A: Mathematical, Physical and Engineering Sciences* 373, 20140375.
12. Fitzenz, D.D., 2018. Conditional Probability of What? Example of the Nankai Interface in Japan. *Bulletin of the Seismological Society of America* 108, 3169–3179.
13. Milner, K.R., Page, M.T., Field, E.H., Parsons, T., Biasi, G.P., Shaw B.E., 2013. Appendix T: Defining the inversion rupture set via plausibility filters, *U.S. Geological Survey Open-File Report 2013-1165-T, and California Geol. Surv. Special Rept. 1792T*, 14 pp.
14. De Risi, R., Goda, K., 2016. Probabilistic Earthquake–Tsunami Multi-Hazard Analysis: Application to the Tohoku Region, Japan. *Front. Built Environ.* 2, 25.
15. The Headquarters For Earthquake Research Promotion, “Tsunami prediction method for earthquakes with specified source faults “Tsunami Recipe”,” 2017, http://www.jishin.go.jp/evaluation/tsunami_evaluation/ (in Japanese).
16. Biasi, G.P., Weldon, R.J., II, Dawson, T.E., 2013. Appendix F: Distribution of slip in ruptures, *U.S. Geological Survey Open-File Report 2013-1165-F, and California Geol. Surv. Special Rept. 228-F*
17. Ellsworth, W.L., Matthews, M.V., Nadeau, R.M., Nishenko, S.P., Reasenber, P.A., Simpson R.W., 1999, A physically-based earthquake recurrence model for estimation of long-term probabilities: *U.S. Geological Survey Open-File Report 99–520*, 22 p.
18. Biasi, G.P., Langridge, R.M., Berryman, K.R., Clark, K.J., Cochran, U.A., 2015. Maximum-Likelihood Recurrence Parameters and Conditional Probability of a Ground-Rupturing Earthquake on the Southern Alpine Fault, South Island, New Zealand. *Bulletin of the Seismological Society of America* 105, 94–106.
19. Abrahamson, N. A., Keuhn, N., Gulerce, Z., Gregor, N., Bozognia, Y., Parker, G., Stewart, J., Chiou, B., Idriss, I. M., Campbell, K. and Youngs, R., 2018. Update of the BC Hydro Subduction Ground-Motion Model using the NGA-Subduction Dataset, *Pacific Earthquake Engineering Research Center (PEER) Technical Report*, PEER 2018/02